Pure & Appl. Chem., Vol. 56, No. 8, pp. 1031-1048, 1984.
Printed in Great Britain.

0033-4545/84 $3.00+0.00
Pergamon Press Ltd.

RECENT APPLICATIONS OF CIRCULAR DICHROISM TO STRUCTURAL PROBLEMS, ESPECIALLY OLIGOSACCHARIDE STRUCTURES

Koji Nakanishi, Masanori Kuroyanagi, Hirofumi Nambu, Eugene M. Oltz, Reiji Takeda, Gregory L. Verdine and Arie Zask

Department of Chemistry, Columbia University, New York, New York 10027, USA

Abstract - First, a brief review of the exciton chirality method is given, with emphasis on practical aspects. This is followed by a case (mitomycin C) in which the interpretation of CD data is purposely carried out in a wavelength region where undesirable interchromophoric interaction is negligible. A new chromophore for coupled CD studies and the additivity relation in coupled CD is mentioned. Generalized schemes for carrying out micro- (μ-) scale structural studies of oligosaccharides, namely identification of sugars and their glycosidic linkages, are described. The simple three-step sequence currently under study is based on the remarkable additivity relationship found in the coupled CD of pyranose p-methoxycarbonyl benzyl ethers.

THE EXCITON CHIRALITY METHOD

The chiral through-space interaction between two or more chromophores gives rise to circular dichroism (CD) curves with extrema of opposite signs ("split CD curve"). The basic theory of this phenomenon was developed in the 1930's by W. Kuhn (coupled oscillator theory, Ref. 1) and J.G. Kirkwood (group polarizability theory, Ref. 2). The application of the coupled oscillator method to various natural products, which we have termed "the exciton chirality method" (Refs. 3 & 4), is in most cases straightforward. Together with the X-ray Bijvoet method, it enables one to determine the absolute configurations of organic compounds without reference to authentic cases; moreover, it can be used for a variety of other purposes besides absolute configurational studies as exemplified by the following attempts to devise microgram scale methods for determining glycosidic linkages in oligosaccharides. Several pertinent points of the exciton chirality method will first be briefly summarized (Refs. 3 & 4). When the symmetric p-substituted benzoate chromophore is close to a chiral center, the strong L_a or intramolecular charge transfer (CT) band gives rise to a CD Cotton effect (CE). In the case of the p-dimethylaminobenzoate (dma-OBz) of cholesterol (Fig. 1, $\underset{\sim}{1}$), the 311 nm UV maximum gives rise to a single CE at 309 nm of moderate intensity. However, when two such chromophores are present in spatial proximity, either intramolecularly or intermolecularly, a through-space interaction takes place and this leads to a CD with extrema of opposite signs (a "split CD"). In the 3,4-dibenzoate case shown, the CE at longer and shorter wavelengths (first and second CE) which have negative and positive signs, respectively, reflect the chirality or screwness between the two L_a electric transition moments. Despite the free rotation around the C-O bond connecting the OBz group to the

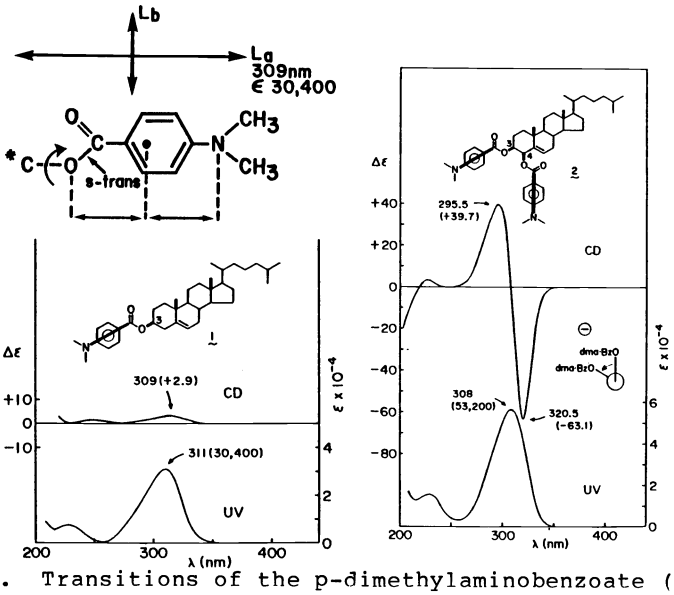

Fig. 1. Transitions of the p-dimethylaminobenzoate (dma-OBz) chromophore and UV/CD of mono- and di-benzoates. Thick bars in 2 show directions of the ^1L_a electric transition moment. The central dot in the phenyl ring represents the point dipole.

carbon atom, the electric transition moments run parallel to the C-O bond because of the s-trans conformation of the ester bond (Fig. 1). The chirality between the two transition moments therefore directly reflects the chirality between the two C-O bonds.

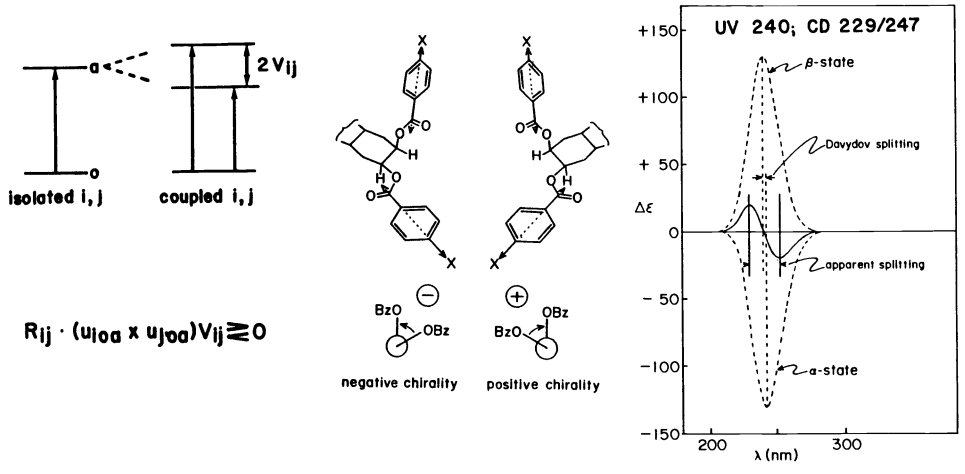

Fig. 2. Nondegenerate system in which chromophoric groups i and j undergo O → a transitions to give split levels separated by $2V_{ij}$.

When the interaction of two (or more) chromophores i and j are chiral, i.e., the two interacting electric transition moments are not in the same plane or do not run parallel, it gives rise to nondegenerate excited electronic levels which are split by $2V_{ij}$, where V is the interaction energy (Fig. 2). The energy gap $2V_{ij}$ is called the Davydov splitting after the physicist who discovered it (Ref. 5). As shown by the dotted curves, the interaction leads to

slightly red- and blue-shifted CD curves of opposite signs which are separated by $2V_{ij}$ (Davydov); the actual split CD curve obtained is represented by the solid curve.

The chirality is defined as negative if the Newman projection of the two dipole moments constitute a left-handed screw when viewed along the line connecting the two carbon atoms and vice versa. Theoretically it is defined by:

$$\vec{R}_{ij} \cdot (\vec{\mu}_{i0a} \times \vec{\mu}_{j0a}) V_{ij}$$

where $\vec{R}_{ij}$ is the interchromophoric distance vector from chromophore i to j, i.e., the distance between the central dots (Fig. 1) of different chromophores, $\vec{\mu}_{i0a}$ and $\vec{\mu}_{j0a}$ are electric transition dipole moments of excitation $0 \rightarrow a$ of groups i and j (obtained from UV/vis oscillator strength), and V_{ij} is the interaction energy (obtained from $\vec{R}_{ij}$, $\vec{\mu}_{i0a}$ and $\vec{\mu}_{j0a}$). When the chirality is negative the sign of the first CE is negative, and vice versa. The coupled CD curves can be readily calculated from the interchromophoric distance and oscillator strength of interacting chromophores and angle between electric transition moments.

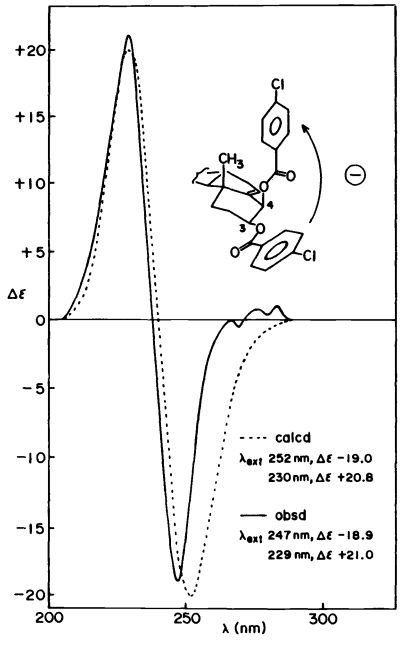

Fig. 3. Observed and calculated CD spectra of cholest-5-ene-3β,4β-diol di-p-chlorobenzoate.

Figure 3 shows that there is excellent agreement between observed and calculated exciton-split CD spectra; in this case the two negatively twisted CT bands of the p-chlorobenzoate chromophore at 240 nm (ε 21,400) give rise to split CD with a negative first and positive second CE at 247 nm (Δε -18.9) and 229 nm (Δε +21.0), respectively. We will define the difference in extrema between the two CE's as the A value; e.g., for the present case it is -39.9, the minus being the sign of the first CE or the chirality. The weak CE's around 280 nm are due to the L_b transition which absorbs at 283 nm (ε 600).

The following aspects should be useful in the application of the exciton chirality method to actual cases:

1. Any chromophore can be used provided the absorption is strong and the direction of μ is known.

2. The stronger the UV ε values, the stronger the A values, i.e., difference between the extrema; as shown in Fig. 4, there is a linear relation between ε and A as the para-substituents in the two benzoate chromophores are changed from $-NO_2$ to $-NMe_2$. Because of the large A values of the dma-OBz chromophore, only μg quantities of sample are needed.

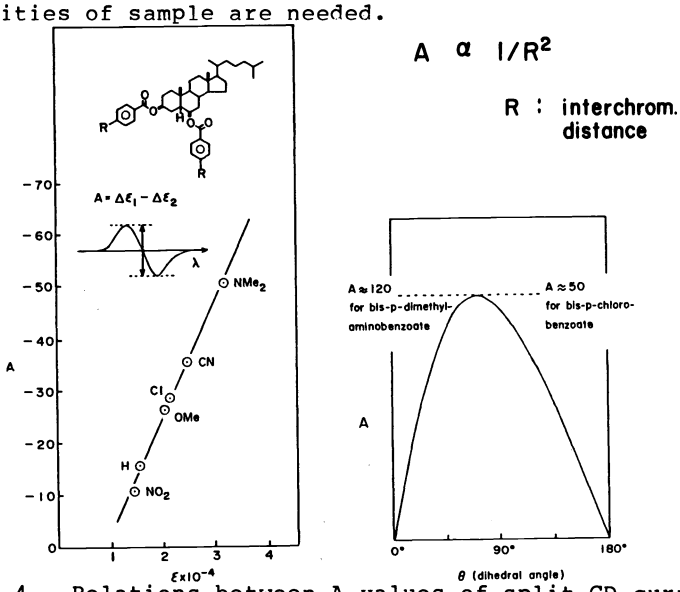

Fig. 4. Relations between A values of split CD curves and (a) ε values; (b) interchromophoric distance R; and (c) dihedral angle of transition dipole moments (calcd.) (Ref. 3).

3. A values are inversely proportional to R or the interchromophoric distance (Fig. 4).

4. Coupling is still observed (A=26) when R is ca. 13Å, i.e., in D-homo-5α-androstane-3β,15β-diol bis-dma-OBz.

5. The A values are maximal around dihedral angels of ca. 70° and zero at 0° or 180°, as calculated for vic-dibenzoates (Fig. 4). Notice the difference in maximal A values of di-p-dimethylamino- and di-p-chloro-benzoates.

6. The sign of the split CD is still retained when the separation in maxima of the two interacting chromophores is 80 nm. In the 3β,4β-dibenzoate shown in Fig. 5 the maximum of the 3-OBz was kept constant while maxima of the 4-OBz were sequentially shifted toward the red by p-substituents. The negative sign of the first CE is still retained in the 6-dma-OBz and excellent agreement between experiment and theory is seen. Only the first CE should be considered since other transitions overlap in the region of the second CE at shorter wavelengths.

7. In multichromophoric systems, the total A value is equal to the sum of interacting units ("additivity relation", see below).

The method has been applied to a variety of natural and unnatural compounds over the past 15 years (Ref. 3). Ongoing studies are discussed in the following section. We start with a case in which the coupled CD region is avoided.

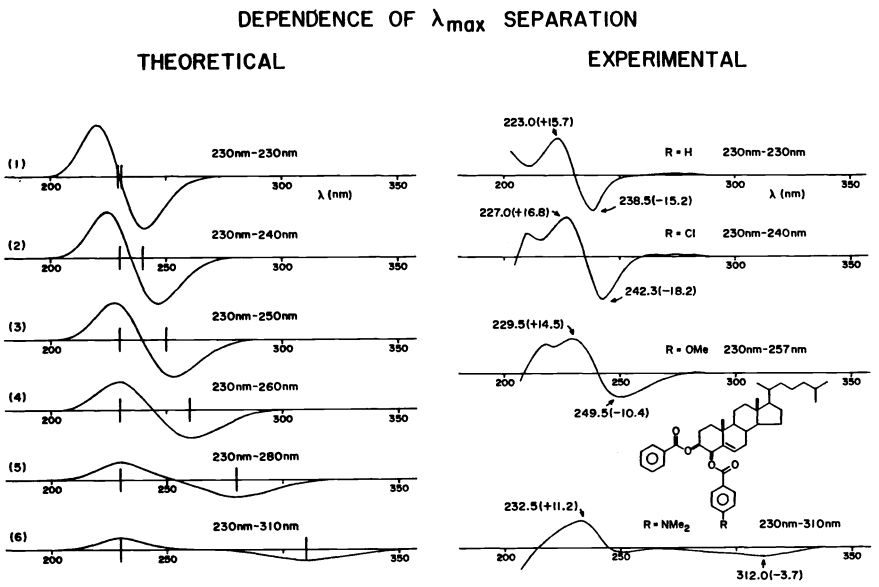

Fig. 5. Dependence of separation in the absorption maxima of two coupled chromophores in cholest-5-ene-3β,4β-diol 3-benzoate 4-p-substituted benzoate.

C-1 CONFIGURATION OF MITOSENES

Mitomycin C (MC, 1, X=NH), the clinically used antitumor drug has been shown to act as a bioreductive alkylating agent (Ref. 6) of DNA (Ref. 7) via cleavage of the 1,2-aziridine ring by HY with concomitant MeOH elimination to yield mitosenes 2 (Fig. 6). This occurs either under acid-catalyzed conditions to give a mixture of 1,2-cis/trans isomers of 2 or under reductive conditions

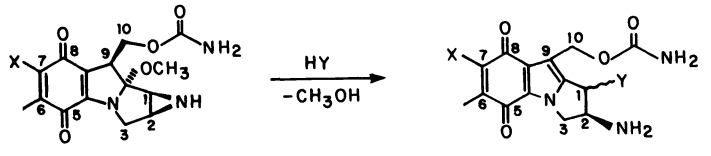

1 2

Fig. 6. Formation of mitosenes by acidic activation or reductive activation.

leading to a predominance of trans-2. Okamoto and co-workers (Ref. 8) were the first to isolate products resulting from interaction of reduced MC with calf thymus MC; in the three adducts the mitosene moiety is linked to O^6 and N-2 of guanylic acid and to N^6 of adenylic acid, with the C-1 configuration unspecified. From the reaction of MC with d(GpC), we had isolated and fully characterized the major adduct 3 to which was assigned a 1-α configuration (Fig. 9) (Ref. 9); a 30 μg-scale differential FT-IR method determined the point of attachment to the guanylic acid moiety (i.e., O^6) whereas a CD method determined the C-1 configuration.

The lack of nonambiguous methods to assign the C-1/C-2 stereochemistry has hampered studies of the aziridine cleavage reactions; it is known that the NMR J values are not reliable (Refs. 9 & 10). The CD method based on the

following rationale provides a direct and general solution to this problem. It also leads to the 1-β structure (Fig. 9, 4) for another adduct produced by the MC/d(GpC) reaction (Ref. 11). The mitosene chromophore is characterized by several optically active absorption bands (Fig. 7) as shown by the weak CE's accompanying the maxima. In the mitomycin C/desoxyguanosine adduct 3, the mitosene and guanosine chromophores both have absorption in the UV region (Fig. 8) and hence the intense CD Cotton effects below 400 nm can certainly be ascribed to coupled-oscillator type interactions.

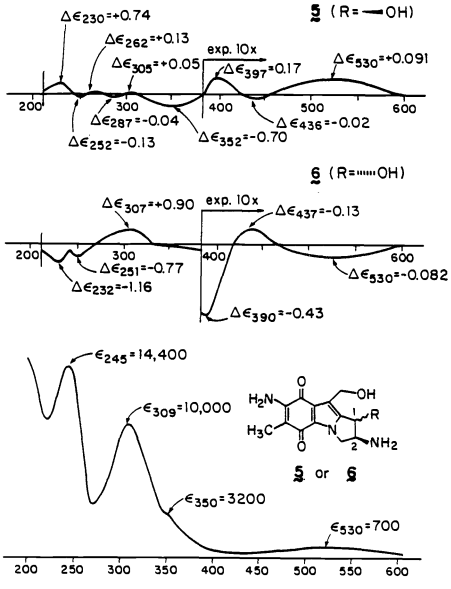

Fig. 7. UV/visible and CD spectra of mitosenes 5 and 6, in MeOH.

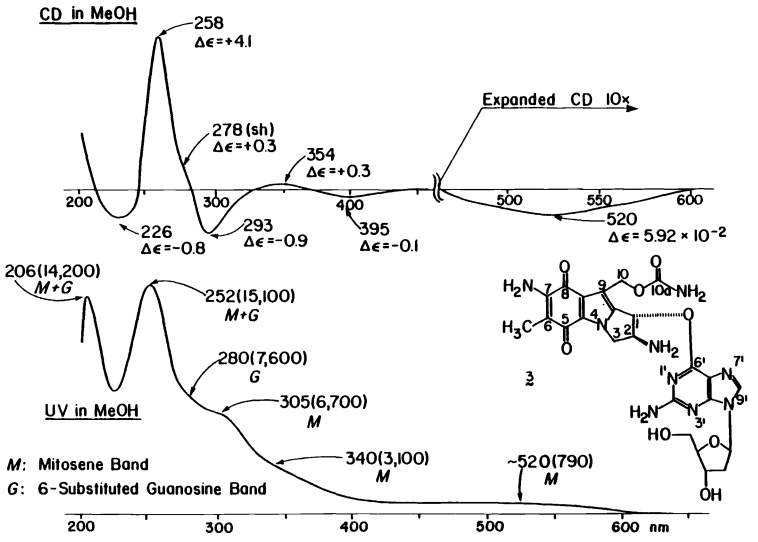

Fig. 8. UV/visible and CD spectra of adduct 3, in MeOH: the M and G denote bands due to the 7-aminomitosene and desoxyguanosine, respectively.

Figs. 7 and 8 show that there is an additional weak but distinct CE at 530 nm corresponding to the 530 nm band, which in turn is responsible for the purple

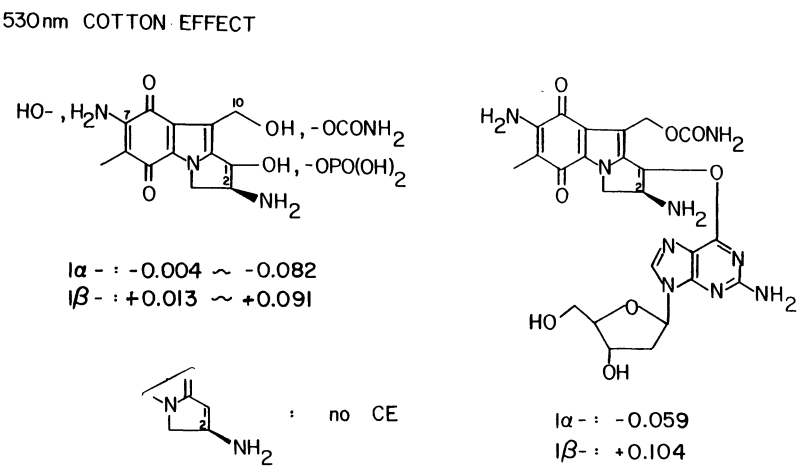

Fig. 9. The 530 nm CE of mitosenes and adducts 3, 4.

color of the mitomycins. It is seen that in 5 with a 1β-OH the sign is positive whereas in 6 with a 1α-OH the sign is negative. The CE is thus due to a perturbation of the 530 nm absorption band by the chiral center at C-1. Four authentic diastereomeric pairs of established 1α/1β-configurations, with 2β-NH_2 and various substituents at C-7, C-10 and C-1 were prepared and the CD were measured. In all cases, 1β and 1α configurations were associated with positive and negative 530 nm CE's, respectively; when C-1 had no substituent the 530 nm CE was also absent (Fig. 9). The sign of this CE can safely be employed to determine the C-1 configuration in adducts 3 and 4 as well. Namely, as demonstrated above (Fig. 5) absorption bands with wide separation in maxima still do interact; however, the 530 nm band of the mitosene moiety is too weak and too far separated from the guanosine 280 nm band and therefore the CE sign only reflects the configuration at C-2. The sign of the 530 nm CE thus provides a simple solution to determine the C-1 configuration.

P-DIMETHYLAMINOCINNAMATE CHROMOPHORE

Since the original absolute configuration of mitomycin C (MC) deduced by x-ray of its heavy atom derivatives was inconsistent with biosynthetic feeding experiments, the X-ray of its 1-N-p-bromobenzoate was re-investigated with sugar; this led to a revision to that shown above (Ref. 12). CD studies with the new chromophore p-dimethylaminocinnamate (dma-OCin) also leads to the same conclusion. Namely, straightforward application of the exciton chirality method to the 1,2-O,N-bisbenzoate should give the absolute configuration. However, since the mitosene chromophore has intense absorptions at 245 nm (ε 14,400), 309 nm (ε 10,000) and a moderate band at 350 nm (ε 3,200) (Fig. 7), the acylate chromophore should be such that the interaction with the mitosene moiety is minimal. The coupling can be suppressed when the separation in maxima is large (Fig. 5) or when the ε of the two acylates are much larger than that of the mitosene group. None of the conventionally used p-substituted benzoates fulfill these criteria. The 1,2-bis-β-naphthoate (237 nm, ε 124,500; chromophore is not strictly symmetric) and the 1,2-biscinnamate

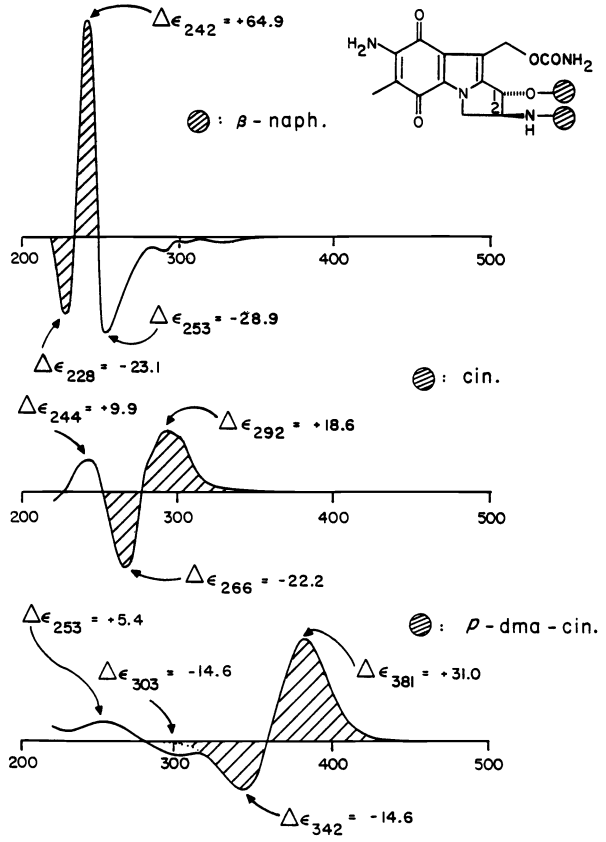

Fig. 10. Exciton-split CD curves of mitosene 1,2-bis-β acylates: (a) bis-β-naphthoate; (b) bis-cinnamate; and (c) bis-p-dimethylaminocinnamate.

do show the positively split CD (Fig. 10a, 10b, shaded area) but they still interact considerably with the mitosene 245 and 309 nm bands. In contrast, the maximum of the bis-dma-OCin chromophore is red-shifted (362 nm, ε 44,000) and also much stronger than the mitosene 350 nm (ε 3,200) band so that interaction between the 1,2-acylates is much more isolated. The positive first CE leads to a positive chirality and hence the revised absolute configuration. Of the several chromophores employed so far in the exciton chirality method, the dma-OCin group is the most red-shifted and its ε is large. The longer wavelength shift to the 360 nm region not only reduces interference from other chromophores but also facilitates CD measurements. Furthermore, in view of the linear relation between the ε and A values of split CD curves, the large means enhanced sensitivity or small sample amount. The chromophore should be promising.

ADDITIVITY RELATION IN A VALUES

Over 40 di-, tri- and tetra-p-bromobenzoates of methyl pyranosides were prepared and the amplitudes (A values) of the split CD curves were measured. It was then found that the A values of tri- and tetra- benzoates could be approximated by the sum of A values of the three and six component dibenzoate units,

respectively (Ref. 13). The set of dibenzoate A values (Fig. 11) thus serve as constants for estimating the A values of any pyranose polybenzoate. It is important that benzoates be measured in MeCN and not in MeOH because ester exchange was noted occasionally in MeOH. In Fig. 11 the "unsubstituted carbons" can be substituted with any group so far as it does not interact (or couple) with the benzoate chromophore; in classes (V) and (VI) the C-4 substituents are also shown even when they are not benzoate groups (cases 9, 10, 11, 13, 14) because the 6-OBz conformation depends on whether the C-4 substituent is eq (glucose) or ax (galactose). As seen in Fig. 12, there is excellent agreement between the observed and calculated A values. Figure 13 lists data for α-methylglycoside per-p-bromobenzoates of pyranoses which are commonly encountered in glycoproteins (Ref. 14). Except for D-GalNAc, again a

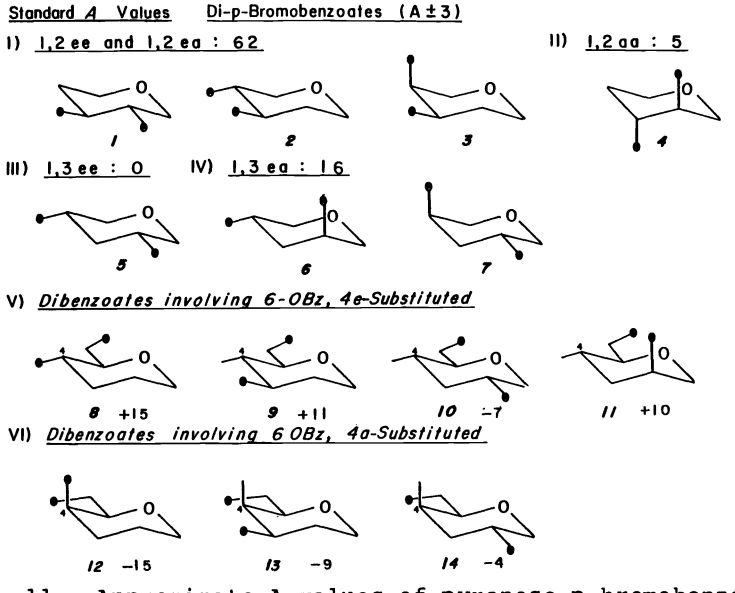

Fig. 11. Approximate A values of pyranose p-bromobenzoates (hatched circles). The anomeric carbon is normally α-OMe but occasionally β-OMe. The "unsubstituted" carbons are either methylenes or substituted with OAc, OMe, Me, CH_2OH, etc.

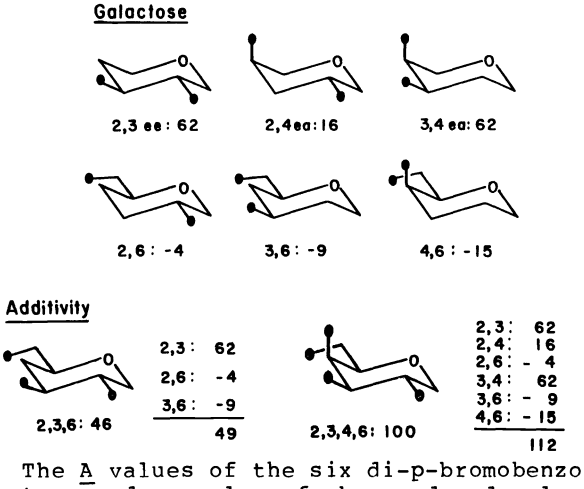

Fig. 12. The A values of the six di-p-bromobenzoate units in D-galactose and examples of observed and calculated A values.

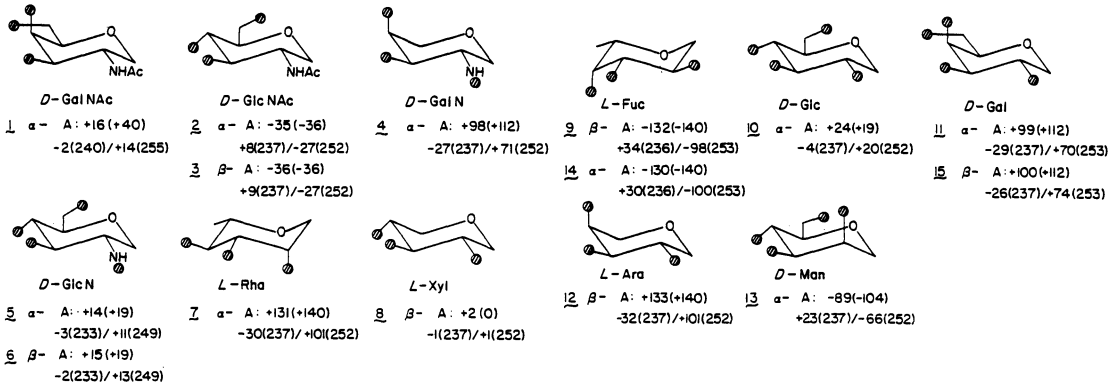

Fig. 13. Observed and calculated (in parentheses) $\underline{A}$ values of methylpyranoside, per-O,N-p-bromobenzoates. The $\overline{\Delta\varepsilon}$ and wavelength (nm, in parentheses) of extrema are also listed. Data measured in MeCN.

remarkable agreement is seen between experimental and calculated values; the origin of the GalNAc disagreement is unknown although it must be related to subtle conformation differences. Note that the additivity relation also holds for -NBz groups, i.e., the values used for OBz are applicable without change. This will clearly simplify further operations in oligosaccharide structure studies.

The additivity relation has been found to hold for benzoate and enone groups present in polyhydroxylated steroidal enones, i.e., ecdysteroids, and other terpenoids as well (Ref. 15). The implication of these findings are far-reaching because they should greatly simplify the CD analysis of multichromophoric compounds. It has been found that this relation still holds for congested cage-structured molecules exemplified by the tricothecenes.

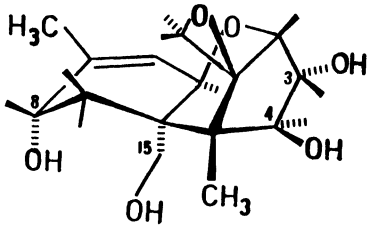

MICRO-SCALE ANALYSIS OF OLIGOSACCHARIDE GLYCOSIDIC LINKAGES

Routine microanalytical techniques are now available for nucleic acids and proteins and these have led to spectacular advances in gene technology. However, despite the importance of polysaccharides in nature, particularly as glycoproteins which occur in enzymes, hormones, lectins, membranes, serum glycoproteins, structural glycoproteins, interferons contained in human leucocytes, etc., the available methodology is unsatisfactory to deal with μg quantities of carbohydrate. In marked contrast to peptide and nucleic acid linkages, the multifunctional nature of monosaccharides which contain multiple hydroxyl and amino groups, etc., of varying configurations introduce enormous variations in saccharide structures. It has been calculated that in trimers consisting of 3 monomers XYZ, the number of isomeric peptides is only 6

whereas that of saccharides is 1,056 (Ref. 16). Consequently, an oligosaccharide structure has to be defined by much more data: identification of monosaccharide sequence, α- or β- at anomeric centers, site of glycosidic linkage of nonbranching sugars and of branching sugars, D- or L-series, etc. Furthermore, for many polysaccharides of interest it is frequently impossible to secure even small quantities of homogeneous material. There is thus an acute need to develop microanalytical techniques.

The conventional methods for polysaccharide analysis (Ref. 17) consists of exhaustive methylation with NaH/DMSO/MeI (Hakomori method, Ref. 18) or with NaH/DMF/MeI (for example as in Ref. 19) followed by methanolysis to a mixture of methoxylated methyl glycosides and identification by GC-MS; alternatively, the fully methylated polysaccharide is hydrolyzed to monosaccharides with aq. TFA, aq. AcOH, etc., silylated and analyzed by GC-MS. The retention time and fragmentation pattern are compared with reference samples, the number of which could be enormous because of all position isomers for each methylated monosaccharide. The methylation analysis is sometimes combined with $NaBH_4$ reduction to alditols and acetylation (Ref. 17). Recent progress in MS has had a great impact on micro-scale structural studies of polysaccharides, especially sequencing (Ref. 20), but configuration isomers cannot be differentiated.

Our current aim is to develop simple micromethods (μg scale where NMR cannot be used) for determining the glycosidic linkage in saccharides up to about decasaccharides. Larger polysaccharides will have to be cleaved specifically or randomly, either by enzymes or by reagents.

Microanalysis of total monosaccharides and identification of branching point pyranoses

The constituent monosaccharide units obtained upon hydrolysis or methanolysis first have to be identified. We described a preliminary account on the HPLC characterization of monosaccharides as their per-p-bromobenzoates in which the anomeric OH groups are also acylated (Ref. 21). However, since methanolysis is the first step in some of the methods for oligosaccharide structure determination currently in use and those under development in our laboratory, more extensive studies were carried out on micro-scale identification of methyl glycosides. This led to the ca. 1 ng-scale HPLC (245 nm detection) identification of pyranoses, pyranoseamines and N-acetylpyranose amines in the form of their methylglycoside O,N-per-p-bromobenzoates (Ref. 14); the α- and β-glycosides give separate peaks but usually one anomer (α-) is produced preponderantly by methanolysis. The high sensitivity is due to the high ε values (Fig. 14).

If further characterization is necessary, the HPLC fractions are evaporated, dissolved in MeCN, and submitted to CD and then MS measurements. Because of the presence of bromine atoms, the strong (usually base peak) $[M+H]^+$ or $[M+NH_4]^+$ peaks in the desorption CI-MS (NH_3 gas) conveniently appear as clusters characteristic of mono-, di-, tri- and tetra-bromobenzoates (Ref. 14). As the ε's of the benzoates are known (Fig. 14), the concentrations of

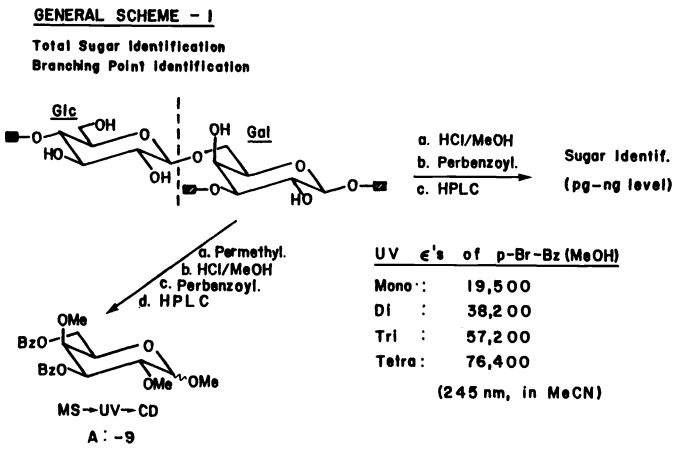

Fig. 14. Microidentification of monosaccharides and determination of branching point pyranose.

solutions submitted to CD can be estimated without weighing. Comparisons of the A values of split CD curves thus obtained with standard values given in Fig. 13 lead to unequivocal characterization of the pyranose ("MS-UV-CD" sequence). The sensitivity of CD measurements necessarily depends on the amplitudes, but in general ca. 100 ng is required with conventional 1-cm path length cells.

The detection sensitivity (250 nm) can be further increased to the 100 pg level by per-2-naphthoylation, yield ca. 80%. The CD amplitudes of the naphthoates were about 10-fold those of the bromobenzoates. Usage of a fluorescence detector will further increase the sensitivity by at least 10-fold.

Thus, in the analysis of sugar residues in oligosaccharides, the sugar is subjected to permethylation, methanolysis, p-bromobenzoylation or pernaphthoylation, and the methyl glycoside peracylates are separated and identified by HPLC. It was applied to 25 μg of viridopentaose C, a pentasaccharide consisting of one D-glucose, two N-acetyl-D-acosamines and two D-quinovoses (Ref. 14). If the methanolysis is preceded by permethylation (with NaH/DMSO/MeI, NaH/DMF/MeI, etc.) and followed by a similar operation sequence, it results in μg-scale determination of glycosidic linkages of pyranoses at branching points. In the hypothetical case shown in Fig. 14, this leads to a dibenzoate with A value of ca. -9. Figure 11 tells us that this should be the 4,6-diOBz derivative of D-Gal; therefore the branching is also 4,6-. The method has been successfully applied to balanitin-1 (100 μg or 0.1 μmole), a saponin, MW 930, with a tetrasaccharide moiety (Ref. 22), and to viridopentaose C (50 μg), a pentasaccharide, MW 1,056 (Ref. 23).

General scheme for determination of sugar and glycosidic linkages

A somewhat cumbersome but general scheme for identifying nonbranching and branching points as well as sugar residues is given in Fig. 15. The oligosaccharide is perbenzylated, methanolyzed and fractionated by HPLC. A

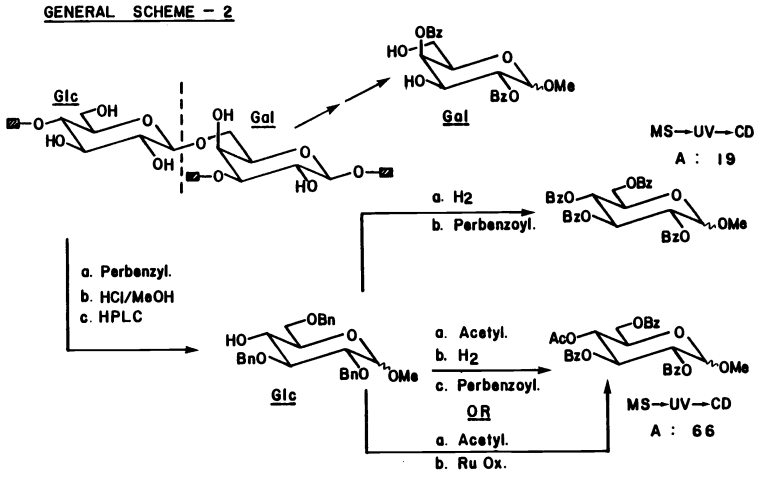

Fig. 15. Procedure for identification of sugar and glycosidic linkages.

portion of the HPLC-separated methylglycoside benzylates (from Glc and Gal in Fig. 15) is hydrogenated with Pd/C to remove the benzyl group and then benzoylated to the methylglycoside perbenzoate for sugar identification. The remainder of the HPLC fraction is: (a) submitted to acetylation to acylate the free hydroxyls which were originally involved in glycosidic linkage; (b) the benzyl groups are removed by hydrogenolysis; and (c) the liberated hydroxyls are perbenzoylated to give sugars benzoylated at positions correspoding to free hydroxyls in the saccharide. The benzoate positions are then determined by the MS-UV-CD sequence.

An alternative simpler procedure is to: (a) acetylate free hydroxyls and (b) oxidize the benzylate to the benzoate mentioned above. We have found that a slightly modified Sharpless procedure (Ref. 24) allows one to oxidize methylglycoside perbromobenzyl ethers (with/without -OAc and -NAc) to corresponding perbromobenzoates efficiently in 70-80% (after prep-TLC purification).

An application of this general scheme to the structure determination of the molluscicidal saponins isolated from the Mexican plant Agave lecheguilla is given in Fig. 16 (unpublished). The sequencing of the oligosaccharide moiety rests on MS results.

Attempts to simplify general scheme

The micro-scale identification of sugar units and determination of glycosidic linkages is based on the high UV ε values and split CD A values of the perbenzoates. Although it can be carried out, the scheme outlined in Figs. 15 and 16 involving protection-deprotection steps is awkward; however, protection-deprotection cannot be avoided because benzoate groups are known to migrate during the vigorous methanalysis step (reflux overnight in MeOH/HCl). Considerable effort was thus directed in the search for symmetric chromophores which would withstand glycoside cleavage conditions and for conditions of milder cleavage reactions. Sugar permesitoates which are less prone to migration were prepared by oligosaccharide permesitoates resisted methanolysis.

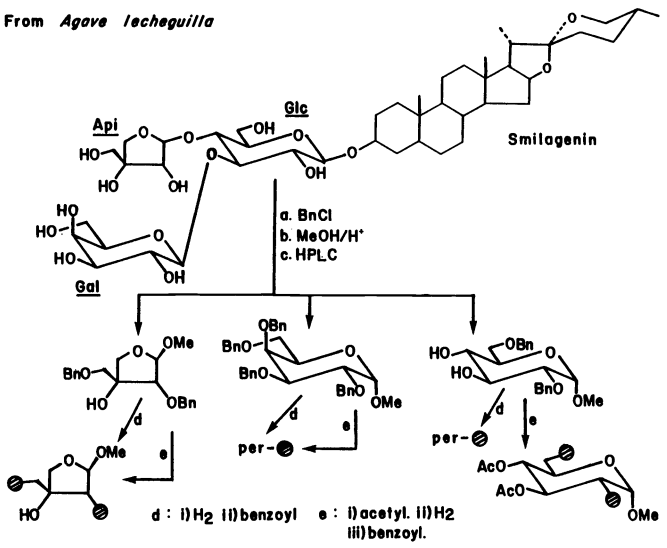

Fig. 16. Determination of sugars and glycosidic linkages in a molluscicidal saponin.

Two schemes which appeared to be promising are shown in Figs. 17 and 18. It was found that 2-methylbenzoate was somewhat less prone to migration and that BF_3-catalyzed mercaptolysis occurred at room temperature. Namely, gentiobiose perbenzoate was cleanly cleaved in 30 min at room temperature with i-PrSH containing BF_3 etherate to give thioacetals which were separated by HPLC; the thioacetals could be reversibly converted into the cyclic thiosugars, the cyclic structure of which renders them amenable to CD analyses, etc. The method was applicable to the larger stachyose peranisoate under similar conditions if the reaction were run for 24 hrs (Fig. 18); the starting anisoates could be produced in quantitative yield by overnight treatment at 60° with the acid chloride in pyridine with a catalytic amount of dimethylaminopyridine.

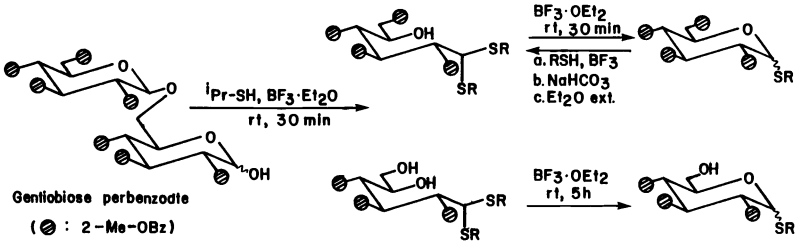

Fig. 17. Mercaptolysis of disaccharide per-2-methylbenzoate.

However, it was found that the reaction proceeded cleanly only for the sterically less crowded 1,6-glycosides. The 1,4-glycosides required more vigorous conditions upon which displacement of benzoates by thioalkyl and other complications resulted. When applied to mixed 1,4- and 1,6-glycosides there was no clear-cut selectivity for 1,6-glycoside linkages and therefore the method could not be employed for selective 1,6-cleavages. The mercaptolysis approach thus had to be abandoned.

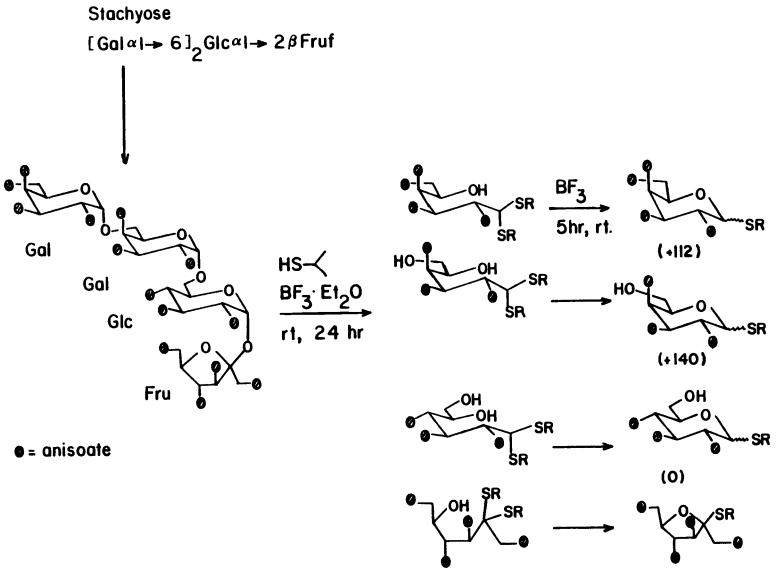

Fig. 18. Mercaptolysis of tetrasaccharide peranisoate.

Additivity relation in A values of benzyl ethers

A breakthrough appears to be the recent finding (unpublished) that the additivity rule found for sugar benzoates is valid for the more flexible benzyl ethers (which are not cleaved by methanolysis or hydrolysis). In order to introduce a chromophore having its electric transition moment parallel to the alcoholic C-O axis, the p-methoxycarbonyl benzyl ether (mcb ether, a reverse benzoate) was employed (Fig. 19). The ε of this chromophore is large

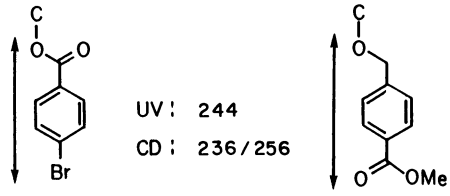

mono	19,500	15,000
di	38,200	30,300
tri	57,200	44,000
tetra	76,400	59,400

in MeCN

Fig. 19. Comparison of p-bromobenzoate and p-methoxycarbonyl benzyl ether (mcb ether).

and the CD of two or more interacting chromophores exhibited typical splitting centered around the UV maximum, i.e., UV 236 nm, CD 224/243 nm (in MeCN) (Fig. 20).

As in the case of pyranose benzoates, a set of standard dibenzyl ethers have been made and the CD A values measured; the A values for D-glucose are listed in Fig. 21 together with A values of corresponding p-bromobenzoates (in parentheses). The smaller A values of mcb ethers are probably due to longer interchromophoric distances arising from their more peripheral locations around

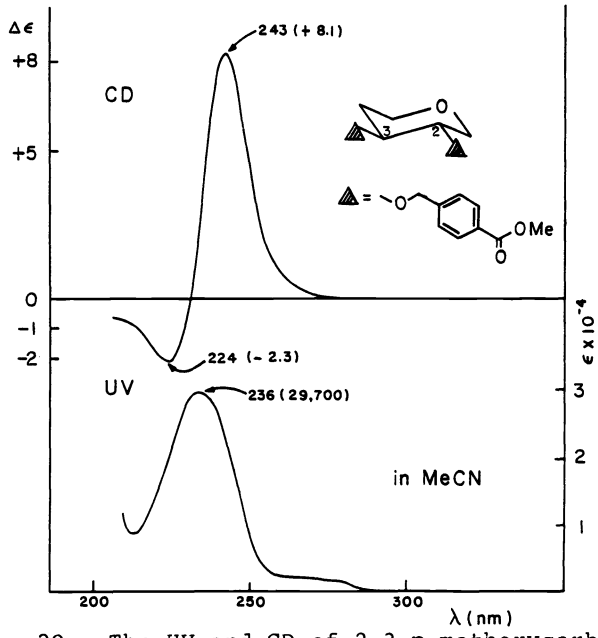

Fig. 20. The UV and CD of 2,3-p-methoxycarbonylbenzyl ether of α-methyl-4,6-diacetoxyglucoside.

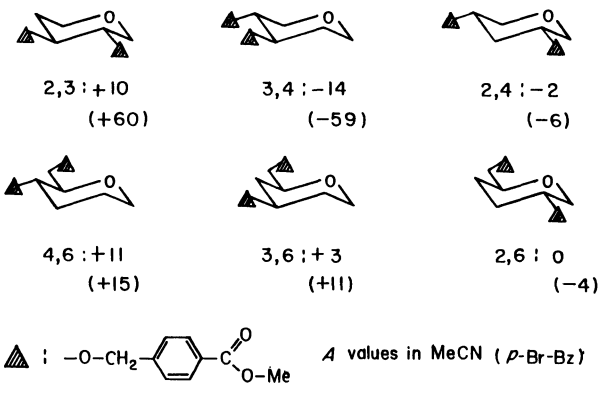

Fig. 21. A values of D-glucose di-mcb ethers and di-bromobenzoates (in parentheses).

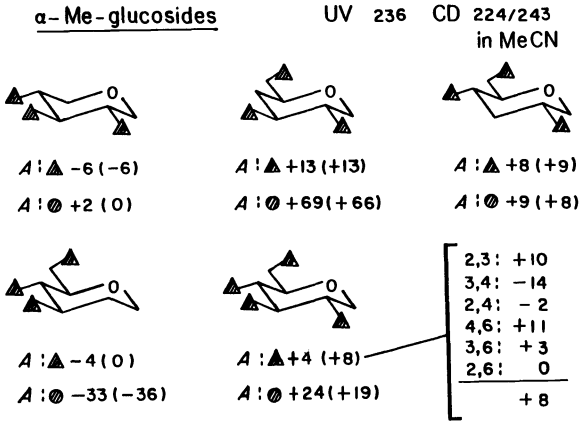

Fig. 22. Observed and calculated (in parentheses) A values. Hatched triangles and circles denote, respectively, the mcb ethers and p-bromobenzoates.

the pyranose ring. It is evident from observed and calculated data for tri- and tetrabenzyl ethers (Fig. 22) that despite the increased possibilities of conformation flexibility, the additivity relation still holds for the benzyl ether chromophore. It is quite remarkable that it is valid for cases involving the 6-benzyl group as well. This agreement between the CD behavior of benzoates and benzyl ethers suggests that the conformation of benzoates is quite rigid and is similar to that of the benzoates; the deduction is supported by MM2 calculations as well (Fig. 23).

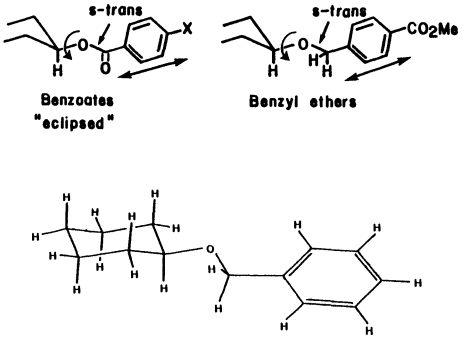

Fig. 23. Conformation of benzoate and benzyl ether. Computed conformation of benzyl ether is also depicted.

Simplified general scheme

This leads to the simplified micro-scale 3-step sequence for characterizing the sugars and glycosidic linkages, branching and nonbranching (Fig. 24):

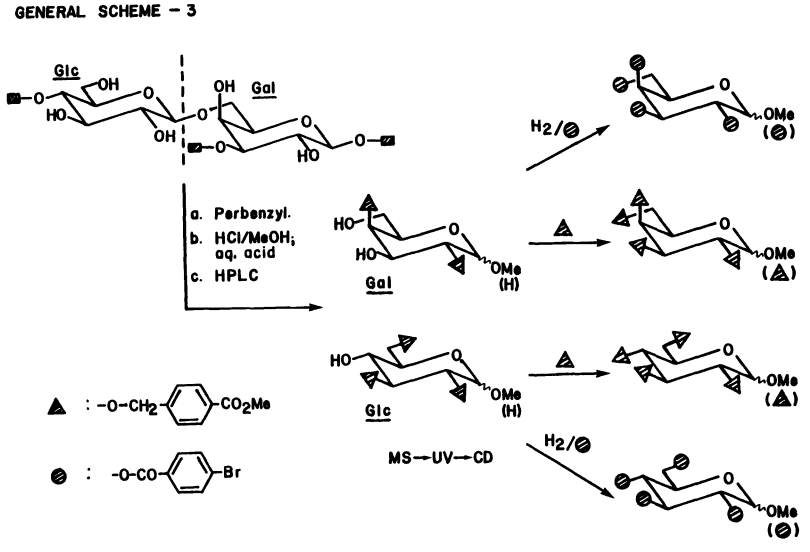

Fig. 24. Simplified general scheme for determination of sugar and glycosidic linkages.

1. The oligosaccharide is perbenzylated, cleaved by methanolysis and the benzyl ethers are separated by HPLC.
2. A portion of the HPLC-separated fraction is submitted to the MS-UV-CD sequence to determine the position of benzyl groups, i.e., free OH in original saccharide, using a list of reference A values for dibenzylates (Fig. 21).
3. Remainder of HPLC fraction is then perbenzylated for sugar identification.

In some cases it may be more convenient to identify the sugar as its glycoside perbenzoate by the hydrogenolysis/perbenzoylation sequence.

4. Formation of α- and β-methyl glycosides (which have to be separated by HPLC) from the same sugar unit by methanolysis can be avoided by hydrolysis with aqueous acetic acid or aqueous trifluoroacetic acid, etc. In this case, the sugar is identified by taking the HPLC peak of the partial benzylates with free anomeric position (α- and β-anomers appear as a single peak) and submitting it to perbenzylation or hydrogenlysis/perbenzoylation; two peaks corresponding to the α- and β-anomeric benzyl ethers or benzoates should be obtained.

The simplified scheme is currently being tested on several oligosaccharides for checking and further refinements.

Acknowledgements - We are indebted to Dr. H.-W. Liu and other colleagues, Drs. M. DiNovi, J. Furukawa, J. Golik, M. Nakatani, R.J. Stonard and D.A. Trainor, who were involved in the early stages of this study (see references cited). These studies are supported by a grant from the National Institues of Health (CA 11572).

REFERENCES

1. W. Kuhn, Trans. Faraday Soc. 26, 293 (1930).
2. J.G. Kirkwood, J. Chem. Soc. 5, 479 (1937).
3. N. Harada and K. Nakanishi, Circular Dichroic Spectroscopy, University Science, California (1983).
4. N Harada and K. Nakanishi, Acc. Chem. Res. 5, 257 (1972).
5. A.S. Davydov, Zhur, Eksptl. i Teoret. Fiz. 18, 210 (1948) [Chem. Abstr. 43, 4575t (1949)]. A.S. Davydov, Theory of Molecular Excitons, Trans. M. Kasha and M. Oppenheimer, Jr., McGraw-Hill, New York (1962).
6. S.-S. Pan, P.A. Andrews, C.J. Glover and N.R. Bachur, J. Biol. Chem. 259, 959 (1984).
7. M. Tomasz and R. Lipman, Biochemistry 20, 5056 (1981).
8. Y. Hashimoto, K. Shudo and T. Okamoto, Tetrahedron Lett. 677 (1982); idem. Chem. Pharm. Bull. 31, 861 (1983).
9. M. Tomasz, R. Lipman, J.K. Snyder and K. Nakanishi, J. Am. Chem. Soc. 105, 2059 (1983).
10. W.G. Taylor and W.A. Remers, J. Med. Chem. 18, 307 (1975).
11. M. Tomasz, M. Jung, G.L. Verdine and K. Nakanishi, submitted for publication.
12. N. Hirayama and K. Shirahata, J. Am. Chem. Soc. 105, 7199 (1983).
13. H.-W. Liu and K. Nakanishi, J. Am. Chem. Soc. 104, 1178 (1982).
14. J. Golik, H.-W. Liu, M. DiNovi, J. Furukawa and K. Nakanishi, Carbohydrate Res. 118, 135 (1983).
15. R.J. Stonard, D.A. Trainor, M. Nakatani and K. Nakanishi, J. Am. Chem. Soc. 105, 130 (1983).
16. N. Sharon and H. Lis, Chem. Eng. News 59, 21 (1981).
17. B. Lindberg, Chem. Soc. Rev. 10, 409 (1981).
18. S.-I. Hakomori, J. Biochem. (Tokyo) 55, 205 (1964).
19. R. Riccio and K. Nakanishi, J. Org. Chem. 47, 4589 (1982).
20. H. Ranvala, J. Finne, T. Krusins, J. Karkkainene and J. Järnefelt, Adv. Carbohydr. Chem. Biochem. 38, 389 (1981).
21. H.-W. Liu and K. Nakanishi, Tetrahedron 38, 513 (1982).
22. H.-W. Liu and K. Nakanishi, J. Am. Chem. Soc. 103, 7005 (1981).
23. M. DiNovi, H.-W. Liu and K. Nakanishi, Tetrahedron Lett. 2485 (1982).
24. P.H.J. Carlsen, T. Katsuki, V.S. Martin and K.B. Sharpless, J. Org. Chem. 81, 3936 (1981); see also P.F. Schuda, M.B. Cishowicz and M.R. Heimann, Tetrahedron Lett. 3829 (1983).